Separation of Liquid Phases in Giant Vesicles of Ternary Mixtures of Phospholipids and Cholesterol

Sarah L. Veatch and Sarah L. Keller
Departments of Chemistry and Physics, University of Washington, Seattle, Washington 98195-1700 USA

ABSTRACT We use fluorescence microscopy to directly observe liquid phases in giant unilamellar vesicles. We find that a long list of ternary mixtures of high melting temperature (saturated) lipids, low melting temperature (usually unsaturated) lipids, and cholesterol produce liquid domains. For one model mixture in particular, DPPC/DOPC/Chol, we have mapped phase boundaries for the full ternary system. For this mixture we observe two coexisting liquid phases over a wide range of lipid composition and temperature, with one phase rich in the unsaturated lipid and the other rich in the saturated lipid and cholesterol. We find a simple relationship between chain melting temperature and miscibility transition temperature that holds for both phosphatidylcholine and sphingomyelin lipids. We experimentally cross miscibility boundaries both by changing temperature and by the depletion of cholesterol with β-cyclodextrin. Liquid domains in vesicles exhibit interesting behavior: they collide and coalesce, can finger into stripes, and can bulge out of the vesicle. To date, we have not observed macroscopic separation of liquid phases in only binary lipid mixtures.

INTRODUCTION

Over the past few years, the fields of membrane biology and biophysics have focused on the role lipids play in membrane organization (Anderson and Jacobson, 2002; Brown and London, 1998; McConnell and Vrljic, 2003; Silvius, 2003). In cell membranes, lipid rafts are currently thought to be localized regions that are on the order of 100 nm in diameter in which certain proteins and lipids are concentrated (Simons and Ikonen, 1997). Both the raft domains and the surrounding lipid matrix are liquid (Pralle et al., 2000). Lipid rafts have been associated with important biological processes such as endocytosis, adhesion, signaling, protein transport, apoptosis, and cytoskeleton organization (Deans et al., 2002; Edidin, 2003; Pike, 2003; Tsui-Pierchala et al., 2002). Since rafts in cell membranes have not been directly observed by standard microscopy, most current assays employ either indirect methods (e.g., detergent resistance), or cross-linking of rafts into larger aggregates (e.g., colocalization) (Thomas et al., 1994).

Lipid-driven lateral separation of immiscible liquid phases is likely a factor in the formation of rafts in cell membranes. Our laboratory and other groups have recently used fluorescence microscopy to directly observe coexisting liquid phases in GUV membranes containing ternary mixtures of saturated lipids, unsaturated lipids, and cholesterol (Dietrich et al., 2001; Samsonov et al., 2001; Veatch and Keller, 2002). This model system has the advantage that large, micron-scale domains can be directly observed by fluorescence microscopy, that miscibility transition temperatures can be measured, and that liquid phases can be studied from a more controlled physical perspective than in cells. Since vesicles can be made without proteins, the lipid contribution to membrane phase separation is isolated. Liquid immiscibility in vesicles has also been probed at smaller length-scales using methods such as FRET and NMR (Vist and Davis, 1990; Wang and Silvius, 2003; Xiaolian and London, 2000).

In earlier work, we varied cholesterol composition against a fixed 1:1 ratio of saturated to unsaturated phospholipids. We observed coexisting liquid phases and mapped the miscibility phase boundary (Veatch and Keller, 2002). Our work left us with clear questions. What are the lipid compositions of the two liquid phases? Over what range in phospholipid compositions are liquid domains observed? To address these questions, we have explored the ternary phase diagram of the saturated lipid DPPC (di(16:0)PC), the unsaturated lipid DOPC (di(18:1)PC), and cholesterol.

Submitted April 28, 2003, and accepted for publication July 9, 2003.

Address reprint requests to Sarah L. Keller, University of Washington, Seattle, WA 98195-1700. Tel.: 206-543-9613; Fax: 206-685-8665; E-mail: slkeller@chem.washington.edu.

Abbreviations used: GUV, giant unilamellar vesicle; FRET, fluorescence resonance energy transfer; Chol, cholesterol; PC, phosphatidylcholine; DCPC, dicaprylphosphatidylcholine (di(10:0)PC); DLPC, dilauroylphosphatidylcholine (di(12:0)PC); DMPC, dimyristoylphosphatidylcholine (di(14:0)PC); DPPC, dipalmitoylphosphatidylcholine (di(16:0)PC); DSPC, distearoylphosphatidylcholine (di(18:0)PC); DAPC, diarachidoylphosphatidylcholine (di(20:0)PC); DOPC, dioleoylphosphatidylcholine (di(18:1) PC); POPC, 1-palmitoyl, 2-oleoylphosphatidylcholine (16:0/18:1 PC); SM, sphingomyelin; BSM, brain sphingomyelin; ESM, egg sphingomyelin; PSM, *N*-palmitoyl-D-sphingomyelin (16:0 SM); SSM, *N*-stearoyl-D-sphingomyelin (18:0 SM).

0006-3495/03/11/3074/10 $2.00

MATERIALS AND METHODS

Commercial reagents

Porcine BSM, SSM, Chol, and all phosphatidylcholine lipids were obtained from Avanti Polar Lipids (Birmingham, AL). PSM and β-cyclodextrin were purchased from Sigma (St. Louis, MO). All lipids were used without further purification, and stock solutions of lipids were stored in chloroform at -20°C until use. Texas Red dipalmitoyl-phosphatidylethanolamine (TR-DPPE, Molecular Probes, Eugene, OR) was used at 0.8 mol % as a dye for contrast between liquid phases. The dye concentration is not crucial. Varying TR-DPPE from 0.2 to 2 mol % in vesicles of 1:1 DOPC/DPPC + 30% Chol produced a scatter in miscibility transition temperatures of <1°C, which is on the order of experimental error.

Vesicles

The methods are as described in Veatch and Keller (2002) and are repeated here. GUVs of diameters 10–50 μm were prepared in >18 MΩ/cm water as described by (Angelova et al., 1992) with modifications to increase yield and compositional uniformity. Specifically, 0.25 mg of lipids were dissolved in chloroform to ~5 mg/ml and spread evenly onto the conducting side of an ITO-coated glass slide. Lipid-coated slides were placed under vacuum for at least 30 min to remove remaining solvent. A capacitor was made from a lipid-coated and uncoated slide coupled with a 0.3-mm Teflon spacer, filled with water, and sealed with vacuum grease. Vesicles were grown for at least 1 h at 60 ± 3°C, then stored warm for at most 2 h before observation. Lipid samples were checked for oxidation by UV/VIS absorption and thin layer chromatography, and no oxidized lipids were detected to within 0.5%. The growth temperature was chosen to be the maximal temperature at which a high yield of GUVs was consistently obtained. Low growth temperatures can result in altered lipid composition. This was observed as a change in transition temperature throughout the sample and was most noticeable near steep regions of the miscibility transition boundary.

Although deposited lipids were uniformly mixed, each vesicle varied slightly in composition. This could be observed as different miscibility transition temperatures and brightness (mol % dye) between vesicles. This composition error is estimated to be <2 mol %. In all cases, we report lipid compositions as prepared in organic solvent before GUV growth. We have not confirmed that resulting GUVs have identical lipid compositions.

To view the sample, vesicle solution was placed between two coverslips and sealed with vacuum grease to prevent evaporation. Heat sink grease was used to thermally couple the coverslip sandwich to a temperature stage. An Alpha-Omega temperature controller was used with a home-built temperature stage consisting of a thermoelectric heater/cooler and a thermistor temperature probe (0.2°C accuracy, Sensor Scientific, Fairfield, NJ). The thermistor was thermally glued to an identical coverslip attached with heat sink grease beside the sample. The same thermistor was used for all experiments, and manufacturer temperature curves were used without further calibration. The accessible temperature range for the sample was between 10°C and 50°C. Epifluorescence microscopy was accomplished with a Nikon Microscope (Melville, NY) with an air objective that did not touch the sample. The depth of field was on the order of 10 μm so that either the top or bottom hemisphere of a vesicle was in focus at one time. Frames were captured with a high sensitivity Photometrics FX CCD camera (Roper Scientific, Tucson, AZ). Transitions were recorded as the temperature at which recognizable domains appeared and then disappeared as temperature was decreased and then increased. Experimental errors in transition temperatures had a systematic contribution of ~±1°C from the response time of the thermistor and a standard deviation from averaging data from at least 10 vesicles. Since miscibility transitions were measured with both increasing and decreasing temperature, error bars represent upper and lower bounds on the true equilibrium miscibility transition temperature even if equilibrium conditions are not met.

Under the microscope, prolonged exposure to light led to photo-oxidation of the few vesicles in the field of view. The effects of photo-oxidation were most noticeable near the miscibility transition and included an increase in the transition temperature and the formation of new, smaller domains in vesicles that were already phase separated. Vesicles that were outside the field of view in the same sample were not affected. To avoid photo-oxidation, transition temperatures were measured by either scanning through temperature at a moderate rate (~0.2°C/s) or stepping at a slow rate (<0.5°C/min) while minimizing light exposure. Both methods produced identical transition temperatures within the reported error bounds.

Potential pitfalls

Although we observe well-defined phase boundaries at some lipid compositions (e.g., between regions B and E in Fig. 2 *a*), we have not established other phase boundaries as precisely and document here all the possible pitfalls for completeness. To start our list, at the boundary between regions D and E, solid and liquid phases are difficult to distinguish when the surface fraction of dark phase is very small (at high DOPC concentrations) and when dark liquid domains are viscous and take long times to become circular (at low cholesterol and/or low temperatures). Similarly, it is difficult to observe solid domains that have elongated into thin lines due to a reduced line tension at increased cholesterol concentration (Korlach et al., 1999). The other side of the diagram, with low DOPC concentration, presents similar difficulties. Small bright phase domains are difficult to distinguish, and domains can take a long time to become circular because viscosity of the dark phase is significant. This is most apparent at low cholesterol and/or low temperatures. In addition, it is likely that a transition to a solid phase exists below the miscibility transition. This transition is challenging to distinguish since our fluorescent probe partitions away from both solid and the ordered liquid phase. At this time, we know of no fluorescent probe in the visible range that preferentially partitions into the ordered liquid phase. Solid transitions were not a focus of this study, but may lead to mischaracterization of liquid coexistence as solid-liquid coexistence when the liquid coexistence temperature range is narrow. Last, as the two-component DPPC-Chol line is approached, the number of DOPC molecules in the bright phase approaches the number of fluorescent probe molecules, which may skew miscibility transition temperatures.

RESULTS

Liquid immiscibility in ternary lipid mixtures

In all cases studied in our laboratory and reported in the literature, GUV membranes that exhibit micron-scale liquid immiscibility contain a minimum of three components: a high melting temperature (saturated) lipid, a low melting temperature (usually unsaturated) lipid, and cholesterol. Table 1 documents all of the lipid mixtures we have tested in GUVs. The first result to note is that most, though not all, of the ternary mixtures produce micron-scale immiscibility over a wide range of temperatures. Next, note that unsaturated lipids are not necessary for micron-scale immiscibility in bilayer membranes. For example, vesicles with DCPC as the low melting temperature component exhibit liquid domains over a range of compositions (Fig. 1 *d*). Finally, note that none of the binary mixtures exhibit micron-scale coexisting liquid phases over the composition and temperature range documented in Table 1.

From this survey, several generalizations can be made:

1. We observe liquid-liquid immiscibility below the melting temperature of the long-chain saturated component in ternary mixtures. We also see that there is a correlation between higher miscibility transition temperatures and higher melting temperature lipids (Samsonov et al., 2001; Veatch and Keller, 2002). The relationship between the main chain transition temperature and liquid immiscibility is remarkably linear for saturated PC lipids in mixtures with DOPC and Chol (Fig. 1 *a*). In addition, transition temperatures in membranes containing pure SM lipids in mixtures with DOPC and Chol fall close to this line.
2. Lipid mixtures containing the asymmetric lipid POPC behave differently from those with DOPC as the

TABLE 1 Miscibility phase behavior for vesicles made from a variety of lipid compositions

Lipid mixture	Ratios	>μm liquid domains?	$T_{miscibility}$	Highest T_m in sample
Binary mixtures				
POPC/Chol	2:1, 4:1	No	–	−2°C
DMPC/Chol	3:1, 17:3	No	–	23°C
D(15:0)PC/Chol	7:3, 17:3	No	–	33°C
DPPC/Chol	3:2, 7:3, 4:1	No	–	41°C
BSM/Chol	2:1, 4:1	No	–	
Ternary mixtures				
DOPC/POPC/Chol	2:2:1	No	–	−2°C
DOPC/DPPC/Chol	1:1:1, 2:1:1, 2:2:1	Yes	29°C, 30°C, 34°C	41°c
POPC/DPPC/Chol	1:1:1, 2:1:1, 2:2:1	No	–	
DOPC/DSPC/Chol	1:1:1, 2:1:1, 2:2:1	Yes	35°C, 38°C, 37°C	55°C
POPC/DSPC/Chol	1:1:1, 2:1:1, 2:2:1	No	–	
DOPC/DAPC/Chol	1:1:1, 2:1:1, 2:2:1	Yes	46°C, 45°C, 47°C	66°C
POPC/DAPC/Chol	1:1:1, 2:1:1, 2:2:1	Yes	–, 33–36°C, 39°C	
DOPC/PSM/Chol	1:1:1, 2:1:1, 2:2:1	Yes	33–35°C, 33°C, 37°C	41°C
POPC/PSM/Chol	1:1:1, 2:1:1, 2:2:1	Yes	16–19°C, 18–20°C, 33°C	
DOPC/SSM/Chol	1:1:1, 2:1:1, 2:2:1	Yes	42–44°C, 39°C, 35–38°C	57°C
POPC/SSM/Chol	1:1:1, 2:1:1, 2:2:1	Yes	23–29°C, 23°C, 35–37°C	
DLPC/DPPC/Chol	2:2:1, 1:3:1	No	–	41°C
DCPC/DPPC/Chol	1:1:1, 2:2:1	Yes	27–33°C, 38°C	
Pseudo-ternary mixtures				
DOPC/ESM/Chol	1:1:1, 2:1:1, 2:2:1	Yes	41–43°C, 38°C, 43°C	39°C
POPC/ESM/Chol	1:1:1, 2:1:1, 2:2:1	Yes	27–29°C, 21–24°C, 33°C	
DOPC/BSM/Chol	1:1:1, 2:1:1, 2:2:1	Yes	24–27°C, 28°C, 37°C	
POPC/BSM/Chol	1:1:1, 2:1:1, 2:2:1	No	–	
Egg PC/BSM/Chol	1:1:1, 2:1:1, 2:2:1	Yes	23–27°C, 28°C, 32–35°C	

Transitions are reported for mixtures that exhibit obvious micron-scale liquid-liquid demixing between 10°C and 50°C. Ranges are given when compositional variations produce >1°C scatter in individual vesicle transition temperatures, indicating that the miscibility boundary is steep (Veatch and Keller, 2003). Main chain transition temperatures were obtained from Silvius (1982) with the exception of PSM (Estep et al., 1979), SSM (Estep et al., 1980), and ESM (Mannock et al., 2003). Mixtures of DPPC/DLPC/Chol were chosen to mimic those reported in Feigenson and Buboltz (2001). Membranes of DAPC/POPC/Chol are viscous, and domains require ~10 min to become circular.

unsaturated component. When phase separation is observed in systems with POPC, miscibility transition temperatures are lower (Fig. 1 *a*) and more dark phase is present (Fig. 1, *b* and *c*). Furthermore, although DOPC/Chol mixtures produce liquid domains when mixed with a wide range of saturated PC lipids (DMPC, di(15:0)PC, DPPC, DSPC, DAPC), POPC/Chol mixtures produce liquid domains only when mixed with the high melting temperature DAPC lipid. Conversely, vesicles made of POPC, Chol, and lower melting temperature SM lipids exhibit coexisting liquid domains over a wide composition range. This significant difference between saturated PC and SM lipids may be due to the availability of hydrogen bond donor and acceptors in the headgroup region of the SM molecule (Brown, 1998). This may be why SM lipids are commonly associated with lipid rafts, given that asymmetric lipids such as POPC are present in large quantities in most biological membranes.

3. Last, miscibility transition temperatures in vesicles containing natural SM extracts (ESM and BSM) are different than would be predicted based on either the chain melting temperature of its major constituent, or on the bulk transition temperature of the lipid extract. This may indicate that contributions from minor components have a large effect on overall membrane phase behavior.

Liquid immiscibility phase boundary for DPPC/DOPC/Chol ternary mixtures

In the following study, we outline the miscibility phase boundary for ternary mixtures of DPPC, DOPC, and Chol. We have chosen the DPPC/DOPC/Chol system for the following reasons:

1. DPPC has been extensively studied in mixtures with cholesterol as well as in mixtures with DOPC (Alecio et al., 1982; Lentz et al., 1976, 1980; McMullen and McElhaney, 1995; Shimshick and McConnell, 1973; Vist and Davis, 1990).
2. DPPC and DOPC share the same phospholipid headgroup, allowing us to focus on the role of the hydrocarbon tails. Table 1 and Fig. 1 suggest that saturated PC and SM lipids behave similarly in mixtures with DOPC.
3. DOPC was chosen over POPC because immiscible liquid phases are observed in vesicles over a wide range of lipid compositions (Table 1). Although POPC is more biologically relevant, its asymmetry could make interpretation of results more difficult.

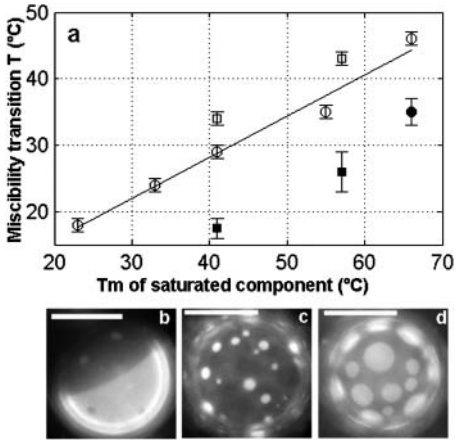

FIGURE 1 (*a*) Plot of miscibility transition temperature versus main chain transition temperature of the saturated component for various ternary mixtures shown in Table 1. Open circle, saturated PC/DOPC/Chol; Open square, pure SM/DOPC/Chol; filled circle, saturated PC/POPC/Chol; and filled square, pure SM/POPC/Chol. Miscibility transition temperatures are from 1:1:1 mixtures with the exception of POPC/DAPC/Chol, which was from a 2:2:1 ratio. Data for DMPC ($T_m = 23°C$) and di(15:0)PC ($T_m = 33°C$) were taken from Veatch and Keller (2002). Line is least squares fit of open circle points and has a functional form of $T_{miscibility} = 0.62\ T_m + 3.4$. (*b–d*) Vesicle micrographs of 1:1:1 mixtures of (*b*) DOPC/SSM/Chol, (*c*) POPC/SSM/Chol, and (*d*) DCPC/DPPC/Chol. All images are taken below the miscibility transition temperature and scale bars are 20 μm.

4. All three components are single lipid species. This allows us to construct a ternary boundary with no ambiguity about the mixture's composition.
5. We are confident that our results presented below for the DPPC/DOPC/Chol system are generally applicable to more biologically relevant mixtures. This is seen in Table 1 and is supported by our previous work on the phase behavior of vesicles containing the ternary mixture egg PC, brain SM, and Chol (Veatch and Keller, 2002). Ongoing work using FRET and fluorescence microscopy to study membranes containing SM, DOPC, and cholesterol is producing similar phase boundaries (Kahya et al., 2003; Smith et al., 2003). In POPC/PSM/Chol mixtures, coexisting liquid domains are observed by FRET at high POPC concentrations presumably due to interactions between POPC and cholesterol (de Almeida et al, 2003).

Phase morphology

The phases we observe in the DPPC/DOPC/Chol system are roughly outlined in Fig. 2 *a*. This map records the first nonuniform phase to be observed at different compositions as temperature is lowered from a high temperature region of one uniform phase. Hence, Fig. 2 *a* contains information about more than one temperature and is not a phase diagram. To make this clear, Fig. 2 *a* is analogous to viewing a hilly landscape from above, rather than taking a cut through that landscape at one elevation.

Fig. 2 *a* contains five distinct regions. We will describe regions A through D before coming to our region of interest, the liquid-liquid coexistence observed in region E. At a high mole fraction, cholesterol is expelled from vesicles such that high cholesterol compositions are inaccessible in region A (Bacha and Wachtel, 2003; Huang et al., 1999). Nevertheless, the majority of the ternary composition space is accessible. Excluding region A and starting at a high temperature above the chain melting temperature of DPPC, all vesicles are observed to be in one uniform liquid phase. As temperature is lowered, the mixtures face four possible outcomes. First, they can remain in one uniform liquid phase as in region B. This occurs when vesicles contain a large fraction of unsaturated lipid (DOPC), greater than 50% Chol, or contain binary mixtures of DPPC and Chol as shown in Fig. 2 *a*, micrographs 2 and 3.

In the three remaining regions (C, D, and E), phases other than one uniform liquid are observed below the chain melting temperature of DPPC. In region C, in the lower right corner of the diagram at large fractions of saturated lipid, lipids are in a solid phase. Traveling left along the DOPC-DPPC axis into region D, there is solid-liquid coexistence. Phase diagrams of similar binary mixtures of high and low temperature phospholipids have been studied both experimentally and theoretically (e.g., Bagatolli and Gratton, 2000, and references therein). Boundaries of the solid-liquid phases can be described in terms of freezing point depression (Ipsen and Mouritsen, 1988). For small increases in cholesterol within region D, the freezing point is further depressed. The coexistence of solid and liquid phases in vesicles and the disruption of solid by higher cholesterol compositions have been documented previously (Feigenson and Buboltz, 2001; Korlach et al., 1999).

The last possible outcome as temperature is lowered is that the vesicle enters a region of coexisting liquid phases (region E). This region is the primary focus of this study. The liquid-liquid coexistence region E is distinguished from the solid-liquid coexistence region D by its domain morphology. Solid domains in region D strongly exclude the fluorescent dye, are generally noncircular, and rotate as rigid bodies in a background of liquid phase (Fig. 2 *a*, micrograph 1). In contrast, we observe that the liquid phases in region E exhibit circular domains that merge by continuously deforming when domains collide (Fig. 3 *a*).

A constant temperature cut through the liquid-liquid coexistence region (region E) is shown in Fig. 2 *b*. We observe that vesicles that contain large fractions of unsaturated lipid (Fig. 2 *b*, micrograph 4) are rich in the bright phase. Increasing the relative amount of saturated lipids and cholesterol at constant temperature increases the surface fraction of the dark phase (Fig. 2 *b*, micrographs 5–8). Micrographs 6 and 7 show vesicles that are near the miscibility transition boundary and have roughly equal area fractions of bright and dark phase. The dotted line that divides region E in Fig. 2 *a* records all compositions for

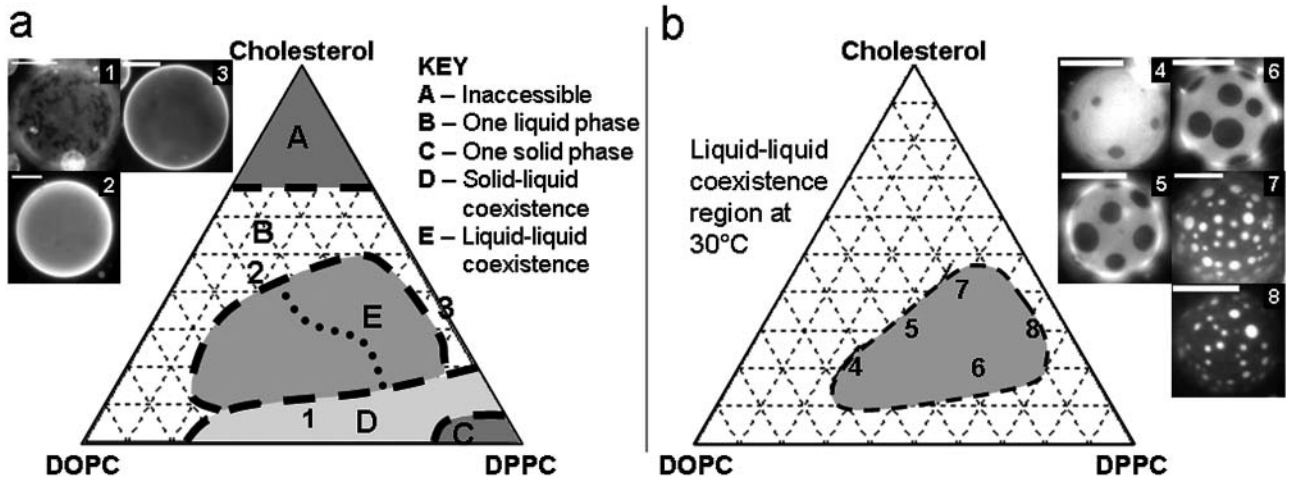

FIGURE 2 (*a*) Sketch of the first phase separation observed in GUVs (if any) as temperature is lowered from a high temperature, one-phase region (see text). This is not a phase diagram since the boundaries are not at a particular temperature. Region E contains vesicles in which a liquid-liquid immiscibility transition is observed. (*b*) Observed phase diagram of micron-scale liquid immiscibility region in GUVs at 30°C. Compositions of vesicles in micrographs 1–8 are as follows: 1), 1:1 DOPC/DPPC + 5% Chol; 2), 2:1 DOPC/DPPC + 45% Chol; 3), DPPC + 40% Chol; 4), 2:1 DOPC/DPPC + 20% Chol; 5), 1:1 DOPC/DPPC + 30% Chol; 6), 1:2 DOPC/DPPC + 20% Chol; 7), 1:2 DOPC/DPPC + 40% Chol; and 8), 1:9 DOPC/DPPC + 30% Chol. All scale bars are 20μm. Vesicles 4–8 were imaged at 30 ± 1°C, and domains are not at equilibrium sizes.

which vesicles possess roughly equal area fractions of bright and dark phase as they pass through the miscibility transition. These observations will be analyzed in more detail in the discussion section.

We know that as temperature is decreased through the miscibility transition, lipid acyl chain order should increase. Indeed, we frequently observe that vesicle area decreases near the miscibility phase transition. Our conclusion that the dark phase is more ordered than the bright phase is supported by two observations. First, as temperature is lowered, the surface fraction of dark phase increases. This increase is monotonic, but not a simple function of temperature, and will be discussed in a subsequent manuscript. Second, bright domains on a dark background diffuse more slowly than dark domains on a bright background. This difference becomes more pronounced at low temperatures.

We observe strong partitioning of TR-DPPE into the less ordered liquid phase over the entire temperature and

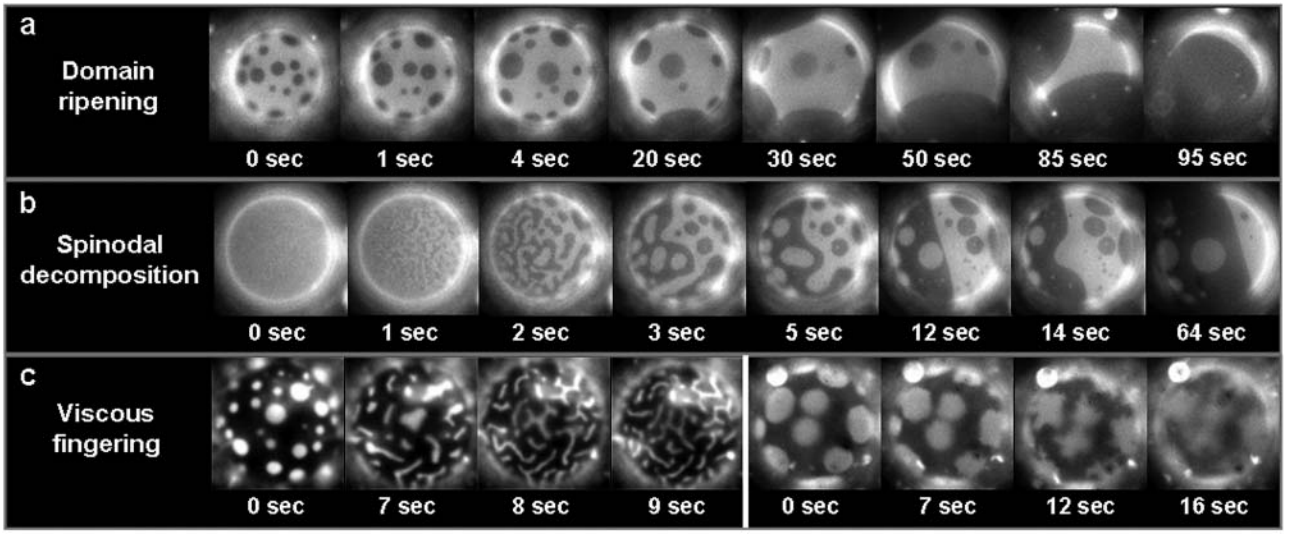

FIGURE 3 Giant vesicles observed near the miscibility transition. (*a*) Domain ripening through time in a vesicle of 1:1 DOPC/DPPC + 25% Chol. Although the proportion of dark phase increases in one hemisphere, it is roughly constant in time over the entire vesicle. (*b*) Time sequence suggesting spinodal decomposition in a vesicle of 1:1 DOPC/DPPC + 35% Chol. (*c*) Viscous fingering in a vesicle of 1:9 DOPC/DPPC + 25% Chol (*left series*) and 1:1 DOPC/DMPC + 25% Chol (*right series*) as temperature is raised through the miscibility transition. The uniform stripe-widths shown at the left are unique to this vesicle composition. All vesicles are roughly 30 μm in diameter.

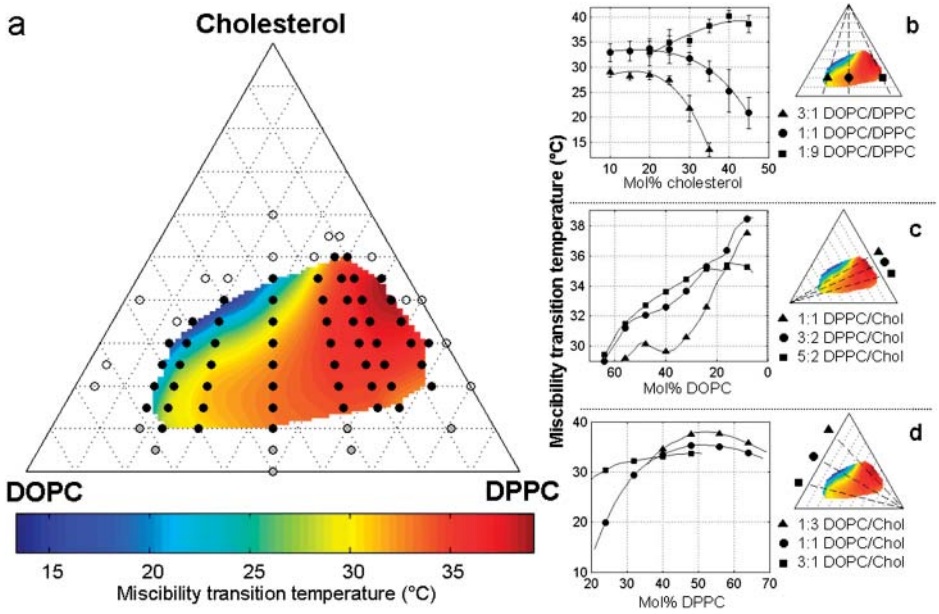

FIGURE 4 Effect of lipid composition on liquid immiscibility transition temperatures in GUVs of DOPC, DPPC, and Chol. (*a*) Open symbols denote that no transition was observed down to 10°C, black symbols denote that miscibility transitions were observed and measured, and gray symbols denote that solid phases were observed. The colored surface is an interpolated fit of the black points. Errors are generally ±1°C. (*b–d*) Two-dimensional cuts through the miscibility phase boundary with constant ratios of (*b*) DOPC/DPPC, (*c*) DPPC/Chol, and (*d*) DOPC/Chol. Actual data points are shown in *b*, and error bars are standard deviations of the temperatures measured. Curves shown in *c* and *d* are cuts through the extrapolated surface, and points do not necessarily represent compositions where temperatures were measured. Solid lines are drawn to guide the eye and are not explicit fits to any theoretical prediction.

composition range explored in this manuscript. Estimates from fluorescent micrographs produce partition coefficients $K_P < 0.4$. This is consistent with results using a similar dye, rhodamine-DMPE, in DMPC/Chol membranes. In that system, the probe also partitioned away from the more ordered state with a coefficient of $K_p = 0.30$ at 30°C (Loura et al., 2001).

Domain kinetics and shapes

Immediately after temperature is lowered into a region of coexisting liquid phases, many small domains are observed. If membranes are given enough time under most experimental conditions, vesicles completely phase separate into a single dark region and a single bright region (Fig. 3 *a*). Domains grow by colliding and coalescing with other domains and not through Ostwald ripening. Merged domains quickly return to a circular shape (Fig. 3 *a*). This indicates that line tension is important and explains why we observe domain sizes comparable to vesicle dimensions (~10 μm). Since the domains are large, bright and dark domains are truly separate phases. When viscosity in the membrane is high, the ripening of domains occurs slowly. We frequently observe slow ripening when the dark phase occupies most of the membrane and the vesicle is at a low temperature. Under these conditions domain size is kinetically trapped at a size smaller than the equilibrium size.

In the special case of vesicles with roughly equal bright and dark surface fractions, domains form via striping as shown in Fig. 3 *b* when temperature is decreased through the transition. This striping is either a kinetic effect caused by spinodal decomposition or an equilibrium effect due to a competition between line tension and long-range repulsive forces in the membrane. Both effects occur near critical points. Spinodal

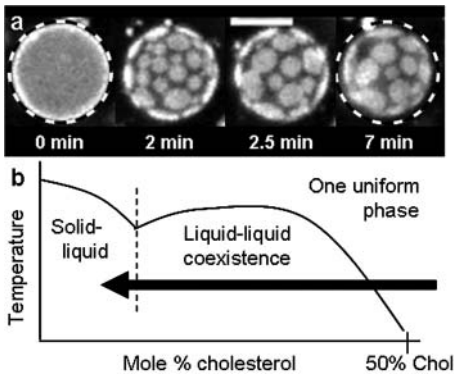

FIGURE 5 (*a*) Time series of 1:1 DOPC/DPPC + 60% Chol vesicle imaged after the addition of β-cyclodextrin (roughly 5 mM) at constant room temperature. Fixed diameter dashed circles demonstrate that the surface area of the vesicle has decreased. Scale bar is 20 μm. (*b*) Sketch of miscibility phase boundary for 1:1 DOPC/DPPC vesicles with varying amounts of cholesterol.

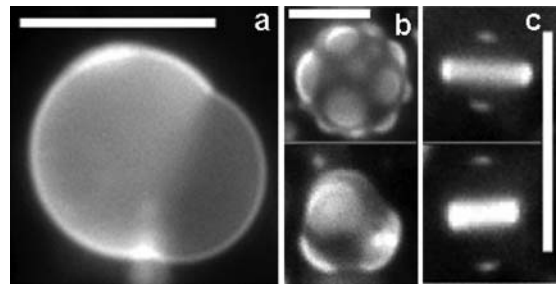

FIGURE 6 Vesicle micrographs of GUVs with bulged domains below their miscibility transition temperature. Vesicles are composed of (*a*) 1:2 DOPC/DPPC + 35% Chol, (*b*) 1:1 DOPC/DMPC + 30% Chol, and (*c*) 1:4 DOPC/DPPC + 25% Chol. All scale bars are 20 μm.

decomposition occurs when a miscible system is quenched below the spinodal curve, leading to fundamental instabilities in the one phase system. Certain wavelength composition fluctuations undergo exponential growth under these conditions, forming domains that are elongated and have a characteristic length-scale (Kahn, 1968). Since line tension is significant, thin elongated domains evolve into thicker stripes and then circles as time progresses (Vlatimirova et al., 1999) (Fig. 3 *b*).

In similar lipid monolayer systems, striping is observed at equilibrium close to a critical point. In these membranes, an interplay between the repulsive dipole interaction and the attractive interfacial line tension leads to stripes of a stable width (Keller and McConnell, 1999). Since photo-oxidation makes it difficult to view a vesicle at a constant offset between the vesicle temperature and the miscibility transition temperature, we cannot definitively test which mechanism is responsible for elongated domains. Evidence against equilibrium striping in bilayers include 1), a lack of a known long-range repulsive force between domains in bilayer membranes, and 2), with the exception of the unique mixture discussed below, uniform striping of domains is not observed when temperature is raised through the miscibility transition.

For the unique case of vesicles with 1:9 DOPC/DPPC + 25% Chol, striped domains are observed when temperature is raised (Fig. 3 *c*, left series). As discussed earlier, such vesicles have bright domains against a background of dark, ordered, viscous phase, and we believe that the stripes are due to viscous fingering. In this membrane, circular domains elongate near the miscibility transition, and stripe widths are uniform throughout the vesicle at each time frame. As time progresses, stripes thin until domains are no longer visible in vesicles. Fingers appear to have uniform widths, and fractal-like branching is not observed. Viscous fingering is also observed in vesicles with low line tension near the miscibility transition, but no uniform stripes are present. For example, the series on the right of Fig. 3 *c* shows that as temperature is raised, multiple thin bright fingers of no uniform width extend into the more viscous dark phase. As time progresses, fingers appear to thin and possibly branch below the resolution of our microscope (1 μm). This dependence of finger width on line tension is consistent with viscous fingering of liquid mixtures in Hele-Shaw cells (Arneodo et al., 1990; Wolf and Woermann, 1998). Further support that these structures are due to viscous fingering is that we do not observe fingering of dark phases into the less viscous bright phase.

Miscibility transition temperature

Fig. 4 shows the miscibility transition temperatures of vesicles of DPPC/DOPC/Chol. It is clear that the miscibility transition temperature is strongly dependent on membrane composition. The highest transition temperatures are found in vesicles rich in saturated lipids and cholesterol whereas vesicles with more unsaturated lipids form two liquid phases only at low temperatures.

It is interesting to study the shape of the phase boundary landscape in Fig. 4. As cholesterol composition is increased in the membranes with more DOPC than DPPC, miscibility transition temperatures decrease continuously until they are below the minimal temperature accessible in our experiments (10°C). This is seen in Fig. 4 *b* (*triangle symbols*). In high cholesterol regions where the miscibility phase boundary is steep, small variations in vesicle composition produce a wide range of transition temperatures and larger error bars (Veatch and Keller, 2003). In contrast, when vesicles contain more DPPC than DOPC, miscibility transition temperatures remain high with small error bars (Fig. 4 *b*, *square symbols*), and suddenly terminate near 50% cholesterol, where domains are no longer observed. A similar abrupt phase boundary can be seen when the DPPC/Chol axis is approached (Fig. 4 *c*). Plotted in three dimensions, the shape of the miscibility transition temperature surface in Fig. 4 *a* resembles a cliff that terminates near the DPPC/Cholesterol binary mixture.

Cholesterol depletion

Although most of this work has focused on using temperature changes to initiate liquid-liquid immiscibility in membranes, the same aim can be achieved by altering the lipid composition of vesicles at a constant temperature. Fig. 5 shows a vesicle that begins with high cholesterol composition in a region of one uniform liquid phase. When β-cyclodextrin is added to the sample, the cholesterol content in the membrane is decreased and the vesicle enters a region of two liquid phases. As expected, bright circular liquid domains move freely on the dark background and then collide and coalesce. At long times, bright domains no longer diffuse even though they remain roughly circular. If, at this point, temperature is raised through the miscibility transition and then lowered back down, noncircular solid domains appear. This indicates that the previous immobile domains may have been kinetically trapped in that configuration (data not shown). Similar micron-scale liquid domains induced by β-cyclodextrin have been observed in living cells (Hao et al., 2001). Our results in model vesicles may provide a framework for interpreting results in biological membranes.

Bulged domains

Domains in vesicles held slightly below the miscibility transition temperature sometimes bulge out of the vesicle surface, as shown in Fig. 6. Both bright and dark domains have been observed to bulge. For some domains, the line boundary between phases decreases in time until each domain is a sphere. This is consistent with the theory that the phase boundary should minimize to decrease the line tension contribution to the free energy (Lipowsky and Dimova,

2003) and is further evidence that line tension is important in this system. Although we do not observe domain budding into the interior of the vesicle, we believe it is possible under different osmotic conditions. We have not further investigated vesicle bulging since we have learned that careful work on this topic is currently being conducted elsewhere (Baumgart et al., 2003).

DISCUSSION

Trends in temperature and composition

It is clear from both Table 1 and Fig. 4 that liquid immiscibility occurs in GUV membranes under a wide range of temperatures and lipid compositions. Although the model ternary compositions we study are too simple to completely represent a biological membrane, we often find miscibility transitions close to physiological temperatures. We speculate that a cell, with more lipids to choose from, could easily tune its lipid composition to be in or near a region of coexisting liquid phases.

We observe two liquid phases, one bright and one dark, in region E of the ternary diagram in Fig. 2. Since we do not know the full composition of each phase, we cannot draw quantitative tie-lines. However, we do know the surface fraction of bright and dark phases in our vesicles. Translating this into a composition of each phase requires knowledge of the molecular area of each species in each phase. This is complicated by the condensing effect of cholesterol and lipids (Phillips, 1972). Nevertheless, from our qualitative results alone, we conclude that the bright phase is enriched in unsaturated lipid (DOPC) and the dark phase is rich in cholesterol and saturated phospholipids (DPPC).

We come to this conclusion by examining vesicles at a constant temperature in Fig. 2 *b*. First, comparing vesicles with equal fractions of cholesterol (20 mol %), the vesicle in micrograph 6 contains more DPPC and more dark phase than the vesicle in micrograph 4. Next, comparing vesicles with equal DOPC/DPPC ratios (2:1) the vesicle in micrograph 7 contains more cholesterol and more dark phase than the vesicle in micrograph 6. Given that our dark phase is rich in saturated lipids and cholesterol, it is likely equivalent to the liquid-ordered state described previously and may resemble detergent resistant phases in biological membranes (London and Brown, 2000).

We use similar logic to estimate the location of tie-lines in Fig. 2 *b*. Micrograph 4 shows a vesicle close to the miscibility transition boundary with a small surface fraction of dark phase. Assuming that there are only two phases present in the liquid-liquid coexistence region at 30°C, the lever rule implies that point 4 must lie near one end of a tie-line. Similarly, vesicles containing more saturated lipids and/or cholesterol contain large surface fractions of dark phase (points 7 and 8) and therefore reside near the opposite end of a tie-line in this picture. This implies that the tie-lines run roughly left to right in the shaded region shown in Fig. 2 *b* with a tilt toward more cholesterol in the DPPC-rich phase.

This tie-line orientation is also supported by our observation of points 5 and 6 in Fig. 2 *b*. Roughly equal surface fractions of bright and dark phase are present in these vesicles near the phase boundary, implying that these vesicles are near a critical composition. Further evidence in these vesicles is that fluctuations in domain boundaries near the miscibility transition are consistent with reduced line tension (as in Fig. 3 *c*, right series), and domains form by a process that resembles spinodal decomposition (as in Fig. 3 *b*). Concluding that points 5 and 6 are near critical points and assuming that only two phases are present in this region, then the tie-lines run roughly left to right with a slope toward more cholesterol in the DPPC-rich phase.

Tie-lines with a shallow slope suggest that cholesterol is more equally distributed between the phases than DPPC is. In fact, our recent results using ^{2}H-NMR to quantify phase composition has shown that DPPC is highly asymmetrically distributed between phases (~80% of DPPCd62 is found in the ordered phase of membranes containing 1:1 DPPCd62/DOPC + 30% Chol at 15°C). Cholesterol is more symmetrically distributed (~2/3 of cholesterol (3 d1) is found in the more ordered phase in membranes of 1:1 DOPC/DPPC + 30% Chol (3 d1) at 20°C) (Veatch et al., 2003).

Comparison with limiting binary systems

The miscibility phase map in Fig. 2 *a* agrees well with previously published phase diagrams for binary mixtures along two of the three edges, for DOPC and Chol as well as for DPPC and DOPC. DOPC and Chol have been shown to mix well down to temperatures below which these experiments were conducted (Lentz et al., 1976). Indeed, we observe that vesicles made of primarily DOPC and cholesterol remain in one uniform phase at 10°C. Mixtures of DPPC and DOPC exhibit an extended gel-liquid coexistence region over the temperature range explored in these experiments (Davis and Keough, 1983). This phase behavior is also reproduced here over a wide temperature and composition range.

The relationship between the results presented in Fig. 2 *a* and previously published phase diagrams for DPPC and Chol membranes is less clear. At first, it seems that these results are in conflict. The lack of observable domains in GUVs with binary lipid compositions is perplexing since many other methods have reported coexisting liquid phases at high temperatures in binary mixtures of DPPC (or DMPC) and Chol. These methods all probe molecular length-scales and include NMR (Vist and Davis, 1990), DSC (McMullen and McElhaney, 1995), ESR (Shimshick and McConnell, 1973), FRET (Loura et al., 2001), fluorescence anisotropy, and freeze fracture (Lentz et al., 1980). By FRET, domain size has been limited to 20 nm at equilibrium in some regions of the liquid-liquid coexistence region of the DPPC/Chol

phase diagram (Loura et al., 2001). This is well below the resolution of optical microscopy, and our results therefore are not in conflict.

This distinction between micron and nanometer scale phase behavior in binary mixtures of DPPC is nontrivial and requires a reexamination of the meaning of phase separation in this context. Certainly, lipid organization on the nanometer length-scale can be a result of two thermodynamic phases that may macroscopically phase separate. However, in some cases it may be a result of dynamic intermolecular interactions that exist within a single phase. For example, surfactants above the critical micelle concentration are considered to be in a single phase even though there is an equilibrium between surfactant monomers and nanometer-scale spherical micelles in solution. In other words, a single spherical micelle is not a separate phase (V. A. Parsegian, personal communication). In lipid monolayer systems, there is also evidence of nanometer-scale organization of saturated lipids and cholesterol in lipid membranes that are not phase separated (McConnell and Radhakrishnan, 2003). Whereas nanometer-scale organization in binary mixtures of DPPC and Chol may not always qualify as a true thermodynamic phase separation, it is probably related to the large-scale liquid immiscibility that we observe in ternary mixtures of DPPC, DOPC, and Chol.

Possible three-phase regions

It is also possible that three-phase regions exist for particular ternary compositions of DPPC, DOPC, and Chol. One candidate region has been proposed by others (de Almeida et al., 2003; Silvius et al., 1996; Smith et al., 2003) and is between the solid-liquid (D) and liquid-liquid (E) regions in Fig. 2 *a*. These two regions could be separated by a uniform liquid phase, a triple point, or an extended region in which three phases are in coexistence, one solid and two liquid. It is also possible that there exists a region of coexistence of three liquid phases in the middle of region E. Since we do not directly observe three-phase coexistence in this experiment, two of these phases would have to be indistinguishable by our fluorescent probe. This is plausible because most ordered phases of DPPC/DOPC/Chol exclude TR-DPPE. To investigate this further by fluorescence microscopy, new probes would have to be discovered that partition well into the liquid phase rich in DPPC and Chol, but not into the solid phase.

CONCLUSION

A clear advantage of working with giant unilamellar vesicles is the ability to directly observe coexisting liquid phases. We find micron-scale liquid domains over a wide range of temperature and lipid composition. The use of simple, model systems allows us to compare results from different methods. We find that no micron-scale phase separation is observed in GUVs of binary lipid mixtures by fluorescence microscopy, whereas nanometer-scale separation is seen by other methods. This suggests that clear, quantitative comparisons between different methods are needed, particularly since so many operational definitions and length-scales for ''rafts'' are currently used (Anderson and Jacobson, 2002). We are currently using NMR to investigate the DPPC/DOPC/Chol system, and our results will appear in a subsequent manuscript.

We thank David Andelman, Harden McConnell, Michael Schick, Kirill Katsov, Ben Stottrup, and Richard Elliott for helpful conversations.

This work was funded by a National Science Foundation CAREER Award (MCB-0133484), a Research Corporation Innovation Award, the University of Washington Royalty Research Fund, and the Petroleum Research Fund. Sarah Veatch was supported in part by a National Institutes of Health predoctoral training grant in molecular biophysics (5T32-GM08268-14) and a National Science Foundation IGERT fellowship from the University of Washington Center for Nanotechnology.

REFERENCES

Alecio, M. R., D. E. Golan, W. R. Veatch, and R. R. Rando. 1982. Use of a fluorescent cholesterol derivative to measure lateral mobility of cholesterol in membranes. *Proc. Natl. Acad. Sci. USA.* 79:5171–5174.

Anderson, R. G., and K. Jacobson. 2002. A role for lipid shells in targeting proteins to caveolae, rafts, and other lipid domains. *Science.* 296:1821–1825.

Angelova, M. I., S. Soleau, P. Meleard, J. F. Faucon, and P. Bothorel. 1992. Preparation of giant vesicles by external AC electric fields. *Prog. Colloid Polym. Sci.* 89:127–131.

Arneodo, A., Y. Couder, G. Grasseau, V. Hakim, and M. Rabaud. 1990. Pattern growth: from smooth interfaces to fractal structures. *In* Nonlinear Evolution of Spatio-Temporal Structures in Dissipative Continuous Systems. F. H. Busse and L. Kramer, editors. Plenum Press, New York. 481.

Bacha, D., and E. Wachtel. 2003. Phospholipid/cholesterol model membranes: formation of cholesterol crystallites. *Biochim. Biophys. Acta.* 1610:187–197.

Bagatolli, L. A., and E. Gratton. 2000. Two photon fluorescence microscopy of coexisting lipid domains in giant unilamellar vesicles of binary phospholipid mixtures. *Biophys. J.* 78:290–305.

Baumgart, T., S. T. Hess, and W. W. Webb. 2003. Imaging coexisting fluid domains in biomembrane models coupling curvature and line tension. *Nature.* In press.

Brown, D. A., and E. London. 1998. Function of lipid rafts in biological membranes. *Annu. Rev. Cell Dev. Biol.* 14:111–136.

Brown, R. E. 1998. Sphingolipid organization in biomembranes: what physical studies of model membranes reveal. *J. Cell Sci.* 111:1–9.

Davis, P. J., and K. M. W. Keough. 1983. Differential scanning calorimetric studies of aqueous dispersions of mixtures of cholesterol with some mixed-acid and single-acid phosphatidylcholines. *Biochemistry.* 22: 6334–6340.

de Almeida, R. F. M., A. Fedorov, and M. Prieto. 2003. A model for raft/non-raft coexistence. Sphingomyelin/phosphatidylcholine/cholesterol phase diagram: boundaries and composition of lipid rafts. *Biophys. J.* 85:2406–2416.

Deans, J. P., H. Li, and M. J. Polyak. 2002. CD20-mediated apoptosis: signalling through lipid rafts. *Immunology.* 107:167–182.

Dietrich, C., L. A. Bagatolli, Z. N. Volovyk, N. L. Thompson, M. Levi, K. Jacobson, and L. A. Gratton. 2001. Lipid rafts reconstituted in model membranes. *Biophys. J.* 80:1417–1428.

Edidin, M. 2003. The state of lipid rafts: from model membranes to cells. *Annu. Rev. Biophys. Biomol. Struct.* 32:257–283.

Estep, T., W. Calhoun, Y. Barenholz, R. Biltonen, G. Shipley, and T. Thompson. 1980. Evidence for metastability in stearoylsphingomyelin bilayers. *Biochemistry.* 19:20–24.

Estep, T., D. Mountcastle, Y. Barenholz, R. Biltonen, and T. Thompson. 1979. Thermal behavior of synthetic sphingomyelin-cholesterol dispersions. *Biochemistry.* 18:2112–2117.

Feigenson, G. W., and J. T. Buboltz. 2001. Ternary phase diagram of dipalmitoyl-PC/dilauroyl-PC/cholesterol: nanoscopic domain formation driven by cholesterol. *Biophys. J.* 80:2775–2788.

Hao, M., S. Mukherjee, and F. R. Maxfield. 2001. Cholesterol depletion induces large scale domain segregation in living cell membranes. *Proc. Natl. Acad. Sci. USA.* 98:13072–13077.

Huang, J., J. T. Buboltz, and G. W. Feigenson. 1999. Maximum solubility of cholesterol in phosphatidylcholine and phosphatidylethanolamine bilayers. *Biochim. Biophys. Acta.* 1417:89–100.

Ipsen, J. H., and O. G. Mouritsen. 1988. Modelling the phase equilibria in two-component membranes of phospholipids with different acyl-chain lengths. *Biochim. Biophys. Acta.* 944:121–134.

Kahn, J. W. 1968. Spinodal decomposition. *Trans. Met. Soc. Am.* 242:166–180.

Kahya, N., D. Scherfeld, K. Bacia, B. Poolman, and P. Schwille. 2003. Probing lipid mobility of raft-exhibiting model membranes by fluorescence correlation spectroscopy. *J. Biol. Chem.* 278:281092–28115.

Keller, S. L., and H. M. McConnell. 1999. Stripe phases in lipid monolayers near a miscibility critical point. *Phys. Rev. Lett.* 82:1602–1604.

Korlach, J., P. Schwille, W. W. Webb, and G. W. Feigenson. 1999. Characterization of lipid bilayer phases by confocal microscopy and fluorescence correlation spectroscopy. *Proc. Natl. Acad. Sci. USA.* 96: 8461–8466.

Lentz, B. R., Y. Barenholz, and T. E. Thompson. 1976. Fluorescence depolarization studies of phase transitions and fluidity in phospholipid bilayers. 2. Two-component phosphatidylcholine liposomes. *Biochemistry.* 15:4529–4537.

Lentz, B. R., D. A. Barrow, and M. Hoechli. 1980. Cholesterol-phosphatidylcholine interactions in multilamellar vesicles. *Biochemistry.* 19:1943–1954.

Lipowsky, R., and R. Dimova. 2003. Domains in membranes and vesicles. *J. Phys. Condens. Matter.* 15:S31–S45.

London, E., and D. Brown. 2000. Insolubility of lipids in triton X-100: physical origin and relationship to sphingolipid/cholesterol membrane domains (rafts). *Biochim. Biophys. Acta.* 1508:182–195.

Loura, L. M. S., A. Fedorov, and M. Prieto. 2001. Fluid-fluid membrane microheterogeneity: a fluorescence resonance energy transfer study. *Biophys. J.* 80:776–788.

Mannock, D. A., T. J. McIntosh, X. Jiang, D. F. Covey, and R. N. McElhaney. 2003. Effects of natural and enantiomeric cholesterol on the thermotropic phase behavior and structure of egg sphingomyelin bilayer membranes. *Biophys. J.* 84:1038–1046.

McConnell, H. M., and A. Radhakrishnan. 2003. Condensed complexes of cholesterol and phospholipids. *Biochim. Biophys. Acta.* 1610:159–173.

McConnell, H. M., and M. Vrljic. 2003. Liquid-liquid immiscibility in membranes. *Annu. Rev. Biophys. Biomol. Struct.* 32:469–492.

McMullen, T. P., and R. N. McElhaney. 1995. New aspects of the interaction of cholesterol with dipalmitoylphosphatidylcholine bilayers as revealed by high-sensitivity differential scanning calorimetry. *Biochim. Biophys. Acta.* 1234:90–98.

Phillips, M. C. 1972. The Physical State of Phospholipids and Cholesterol in Monolayers, Bilayers, and Membranes. Progress in Surface and Membrane Science. Academic Press, New York. 139–221.

Pike, L. J. 2003. Lipid rafts: bringing order to chaos. *J. Lipid Res.* 44:655–667.

Pralle, A., P. Keller, E. L. Florin, K. Simons, and J. K. H. Horber. 2000. Sphingolipid-cholesterol rafts diffuse as small entities in the plasma membrane of mammalian cells. *J. Cell Biol.* 148:997–1007.

Samsonov, A. V., I. Mihalyov, and F. S. Cohen. 2001. Characterization of cholesterol-sphingomyelin domains and their dynamics in bilayer membranes. *Biophys. J.* 81:1486–1500.

Shimshick, E. J., and H. M. McConnell. 1973. Lateral phase separations in binary mixtures of cholesterol and phospholipids. *Biochem. Biophys. Res. Commun.* 53:446–451.

Silvius, J. R. 1982. Thermotropic Phase Transitions of Pure Lipids in Model Membranes and Their Modifications by Membrane Proteins. Lipid-Protein Interactions. John Wiley, New York.

Silvius, J. R. 2003. Role of cholesterol in lipid raft formation: lessons from lipid model systems. *Biochim. Biophys. Acta.* 1610:174–183.

Silvius, J. R., D. del Giudice, and M. Lafleur. 1996. Cholesterol at different bilayer concentrations can promote or antagonize lateral segregation of phospholipids of differing acyl chain length. *Biochemistry.* 35:15198–15208.

Simons, K., and E. Ikonen. 1997. Functional rafts in cell membranes. *Nature.* 387:569–572.

Smith, A. K., J. Buboltz, C. H. Spink, and G. W. Feigenson. 2003. Ternary phase diagram of the lipid mixture sphingomyelin/DOPC/cholesterol. *Biophys. J.* 84:372a. (Abstr.)

Thomas, J. L., D. Holowka, B. Baird, and W. W. Webb. 1994. Large-scale co-aggregation of fluorescent lipid probes with cell surface proteins. *J. Cell Biol.* 126:795–802.

Tsui-Pierchala, B. A., M. Encinas, J. Milbrandt, and E. M. J. Johnson. 2002. Lipid rafts in neuronal signaling and function. *Trends Neurosci.* 25:412–417.

Veatch, S. L., K. Gawrisch, and S. L. Keller. 2003. Observing immiscible liquid phases in lipid bilayers containing cholesterol by fluorescence microscopy and NMR. Biophys. J. (Annual Meeting Abstracts) 83:1806-Pos.

Veatch, S. L., and S. L. Keller. 2002. Lateral organization in lipid membranes containing cholesterol. *Phys. Rev. Lett.* 89:268101.

Veatch, S. L., and S. L. Keller. 2003. A closer look at the canonical ''Raft Mixture'' in model membrane studies. *Biophys. J.* 84:725–726.

Vist, M. R., and J. H. Davis. 1990. Phase equilibria of cholesterol/dipalmitoylphosphatidylcholine mixtures: 2H nuclear magnetic resonance and differential scanning calorimetry. *Biochemistry.* 29:451–464.

Vlatimirova, N., A. Malagoli, and R. Mauri. 1999. Two-dimensional model of phase segregation in liquid binary mixtures. *Phys. Rev. E.* 60:6968–6977.

Wang, T., and J. R. Silvius. 2003. Sphingolipid partitioning into ordered domains in cholesterol-free and cholesterol-containing lipid bilayers. *Biophys. J.* 84:367–378.

Wolf, H., and D. Woermann. 1998. Viscous fingering at the liquid/liquid interface between two coexisting phases of mixtures with a miscibility gap. *Ber. Bunsenges. Phys. Chem.* 102:1783–1793.

Xiaolian, X., and E. London. 2000. The effect of sterol structure on membrane lipid domains reveals how cholesterol can induce lipid domain formation. *Biochemistry.* 39:843–849.